American Mineralogist, Volume 84, pages 718–724, 1999

Crystal growth mechanisms in miarolitic cavities in the Lake George ring complex and vicinity, Colorado

DANIEL E. KILE* AND D.D. EBERL

U.S. Geological Survey, 3215 Marine Street, Boulder, Colorado, 80303-1066, U.S.A

ABSTRACT

The Crystal Peak area of the Pikes Peak batholith, near Lake George in central Colorado, is world-renowned for its crystals of amazonite (the blue-green variety of microcline) and smoky quartz. Such crystals, collected from individual miarolitic pegmatites, have a remarkably small variation in crystal size within each pegmatite, and the shapes of plots of their crystal size distributions (CSDs) are invariably lognormal or close to lognormal in all cases. These observations are explained by a crystal growth mechanism that was governed initially by surface-controlled kinetics, during which crystals tended to grow larger in proportion to their size, thereby establishing lognormal CSDs. Surface-controlled growth was followed by longer periods of supply controlled growth, during which growth rate was predominantly size-independent, consequently preserving the lognormal shapes of the CSDs and the small size variation. The change from surface- to supply controlled growth kinetics may have resulted from an increasing demand for nutrients that exceeded diffusion limitations of the system. The proposed model for crystal growth in this locality appears to be common in the geologic record, and can be used with other information, such as isotopic data, to deduce physico-chemical conditions during crystal formation.

INTRODUCTION

Attempts to model crystal nucleation and growth from classic kinetic theory have been disappointing (Ohara and Reid 1973; Mullin 1974; Dowty 1980; Kirkpatrick 1981; Lasaga 1982). Population balance methods (Randolph and Larson 1988; Marsh 1988; Cashman and Marsh 1988; Cashman and Ferry 1988; Marsh 1998) used by chemical engineers and geologists to model growth often fail to predict accurately the shapes of crystal size distributions (CSDs; Larson et al. 1985), and have been criticized on theoretical grounds (Kerrick et al. 1991; Lasaga 1998). Until recently, there has been no theory, model or simulation method that accounts for all of the following aspects of crystal growth that are commonly observed in crystal growth experiments (Randolph and Larson 1988) and in some natural systems (Nordeng and Sibley 1996): (1) size dispersion, during which crystals initially having the same size may grow at different rates; (2) size dependent growth, during which larger crystals tend to grow faster; and (3) a lognormal shape for many CSDs.

Recently, an approach was developed (Eberl et al. 1998) that simulates these three phenomena, which suggests that crystal growth mechanisms can be deduced from the shapes of CSDs and from the evolution of the parameters α and β^2 during growth. Alpha is the mean of the natural logarithms of the crystal sizes, defined as:

$$\alpha = \Sigma \ln(X) f(X), \quad (1)$$

and β^2 is the crystal size variance, defined as:

$$\beta^2 = \Sigma [\ln(X) - \alpha]^2 f(X), \quad (2)$$

where $f(X)$ is the observed frequency of crystal dimension X. After α and β^2 have been calculated from measured sizes, the theoretical lognormal frequency distribution $g(X)$ can be calculated from (Koch and Link 1971):

$$g(X) = \left[\frac{1}{X\beta\sqrt{2\pi}}\right] \exp\left[-\left(\frac{1}{2\beta^2}\right)[\ln(X) - \alpha]^2\right]. \quad (3)$$

The theoretical curve then can be compared with the measured distribution by using statistical tests to determine if the measured distribution is lognormal.

The present study assesses CSD shape, mean size, and variance to determine crystal growth mechanisms for microcline (variety amazonite; Fig. 1a) and for quartz (variety smoky; Fig.1b) found within miarolitic cavities in the Crystal Peak area in central Colorado. Finding the crystal growth mechanism may be the first step in deducing geologic history from crystals.

REGIONAL GEOLOGY

The Pikes Peak batholith (PPB), primarily a granite to quartz monzonite, is exposed over an area of about 5000 km^2 in central Colorado. It is a Precambrian, anorogenic, epizonal intrusive with an age of 1074–1092 Ma based on recent studies by Unruh et al. (1995). Within this batholith are numerous plutons of sodic and potassic affinity (Wobus and Anderson 1978; Wobus and Hutchinson 1988) that have been mapped by Bryant et al. (1981); miarolitic pegmatites are concentrated in and around these late plutons.

*E-mail: dekile@usgs.gov

0003-004X/99/0506–0718$05.00

The Lake George ring complex (LGR), one of the largest of these late intrusives, is located in the southern part of the PPB; it represents a sequential series of intrusions, from a medium-grained granite at the margin, to an intermediate, fine-grained granite, and finally a centrally located syenite. The well-known pegmatites in the Crystal Peak area (located in Teller and Park counties) are centered in and around this structure.

Miarolitic pegmatites typically show a zonal structure with a central cavity; such cavities form from exsolution of an aqueous vapor phase during crystallization of silicate melt within the pegmatitic structure. A typical miarolitic cavity in the PPB is characterized by an outer zone of graphic granite, followed inward by increasingly larger anhedral crystals (generally elongated and oriented radially toward the center of the pegmatite), and finally by a clay-filled cavity that contains euhedral crystals of microcline, smoky quartz, and other minerals, such as albite, goethite, and fluorite.

EXPERIMENTAL METHODS

Between 1978 and 1992, crystals were collected from eight miarolitic cavities within parent coarse-grained granite (Ypc) of the PPB near or adjacent to the LGR, and from the medium-grained granite (Ypm) comprising part of the LGR, where Ypc and Ypm refer to the map units of Wobus and Anderson (1978**)**. Crystal size distributions were measured using a ruler or a stereomicroscope with a calibrated micrometer ocular for the amazonite variety of microcline and for the smoky quartz crystals that occur within these miarolitic cavities (the 1986 and 1987 miarolitic cavities contained both microcline and quartz; results are shown for each). Only cavities whose entire contents were archived were used in this study; those with only partial contents available are assumed to give biased results with respect to mean crystal size. Further limitations are imposed by the minimum number of crystals within the cavities; only cavities yielding > ~150 crystals of microcline or quartz were assumed to give a statistically valid sampling. Individual crystal size was measured by linear dimension, as the occurrence of intergrown crystals on matrix prevents measurement on a weight basis. Microcline crystals were measured along the *b*-axis, where the predominant cleavage along the (001) plane would not affect overall measurement of otherwise relatively equant crystals. Because the habit of quartz within a given miarolitic cavity is relatively consistent (i.e., length to width ratio), length was assumed to give a reliable measure of crystal size. Crystal sizes were entered into a computer program that compiles the data into selected group sizes and plots them as a size distribution. A theoretical lognormal curve calculated from this data is compared with the curve derived from the experimental data.

Statistical analysis for lognormal fit was done using both the chi-square (χ^2; Krumbein and Graybill 1965) and Kolmogorov-Smirnov (K-S; Benjamin and Cornell 1970) tests. The χ^2 test, which gives a significance level ranging from <1% (not significant) to >20% (high level of significance), was used to compare differential curves of theoretical lognormal vs. measured distributions. The K-S test, which gives a "goodness-of-fit" assessment based on maximum deviation of observed values from a theoretical (lognormal) model, with 5% representing the critical level of significance, was used to compare cumulative distributions.

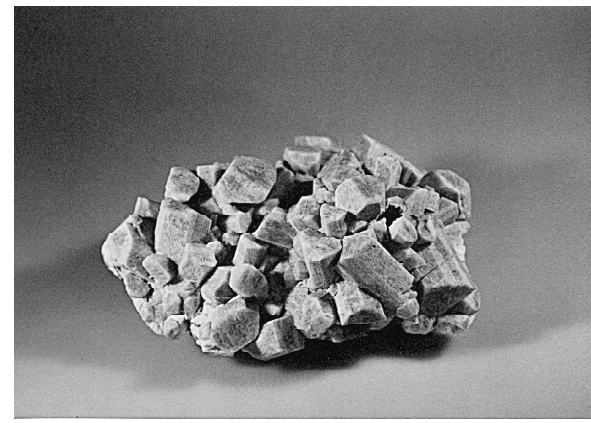

FIGURE 1a. Microcline (variety amazonite) crystal group from the LGR, 1984, illustrating uniform crystal size distribution (i.e., low β^2). Specimen is 18 cm across.

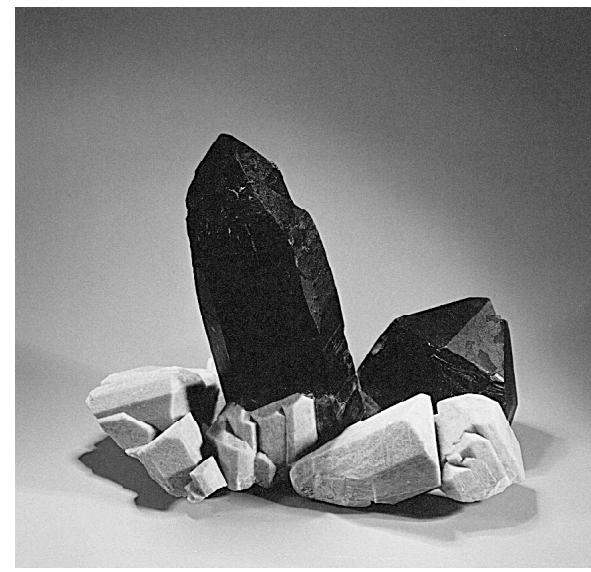

FIGURE 1b. Quartz (variety smoky) and microline (variety amazonite) crystal group from the LGR, 1987, illustrating a uniform crystal size distribution for microcline, and a comparatively larger crystal size variance for quartz. Specimen 22.5 cm high; photo by John R. Muntyan.

EXPERIMENTAL RESULTS

The shapes of CSDs of both microcline and quartz crystals from the studied miarolitic cavities have lognormal or nearly lognormal size distributions as determined by the χ^2 and K-S tests (Table 1 and Fig. 2). Furthermore, a plot of the α and β^2 values for microcline crystals from each of the pockets shows a relatively constant and small crystal size variation (β^2) over a range of mean size that spans more than an order of magnitude (i.e., mean sizes from 1.4 mm to 44 mm), whereas quartz shows a somewhat larger β^2 for a smaller range of mean size (Fig. 3a).

TABLE 1. Pegmatite crystal size distribution data and statistical evaluation

Mineral/Pegmatite	α	β^2	Level of significance (%) χ^2 test	Level of significance (%) K-S test	Mean crystal size (mm)	No. crystals
Microcline (var. amazonite)						
LGR/Ypc, 1978	16.9	0.18	>20	>10	24.3	174
LGR/Ypc, 1984	16.4	0.12	<1	1–5	14.6	747
LGR/Ypm, 1985	16.7	0.08	>20	>10	18.1	182
LGR/Ypc, 1986	17.0	0.10	>20	>10	27.0	315
LGR/Ypc, 1987	17.5	0.12	<1	>10	43.9	193
LGR/Ypc, 1989	17.4	0.11	>20	>10	37.1	216
north of LGR, 1992	14.1	0.15	10-20	>10	1.41	454
Quartz (var. smoky)						
LGR/Ypm, 1985	17.6	0.29	>20	>10	50.4	197
LGR/Ypc, 1986	18.0	0.26	2.5-5	>10	77.5	177
LGR/Ypc, 1987	17.9	0.36	2.5-5	>10	75.4	192

Notes: LGR = Lake George ring; Ypc and Ypm = coarse-grained and medium-grained granite, respectively, and indicate the host granite in which the pegmatite was located; date indicates year pegmatite collected. Computation of α and β^2 values based on crystal size expressed in nanometers. LGR/Ypc, 1986 and LGR/Ypc, 1987 microcline and quartz data are from the same miarolitic cavity.

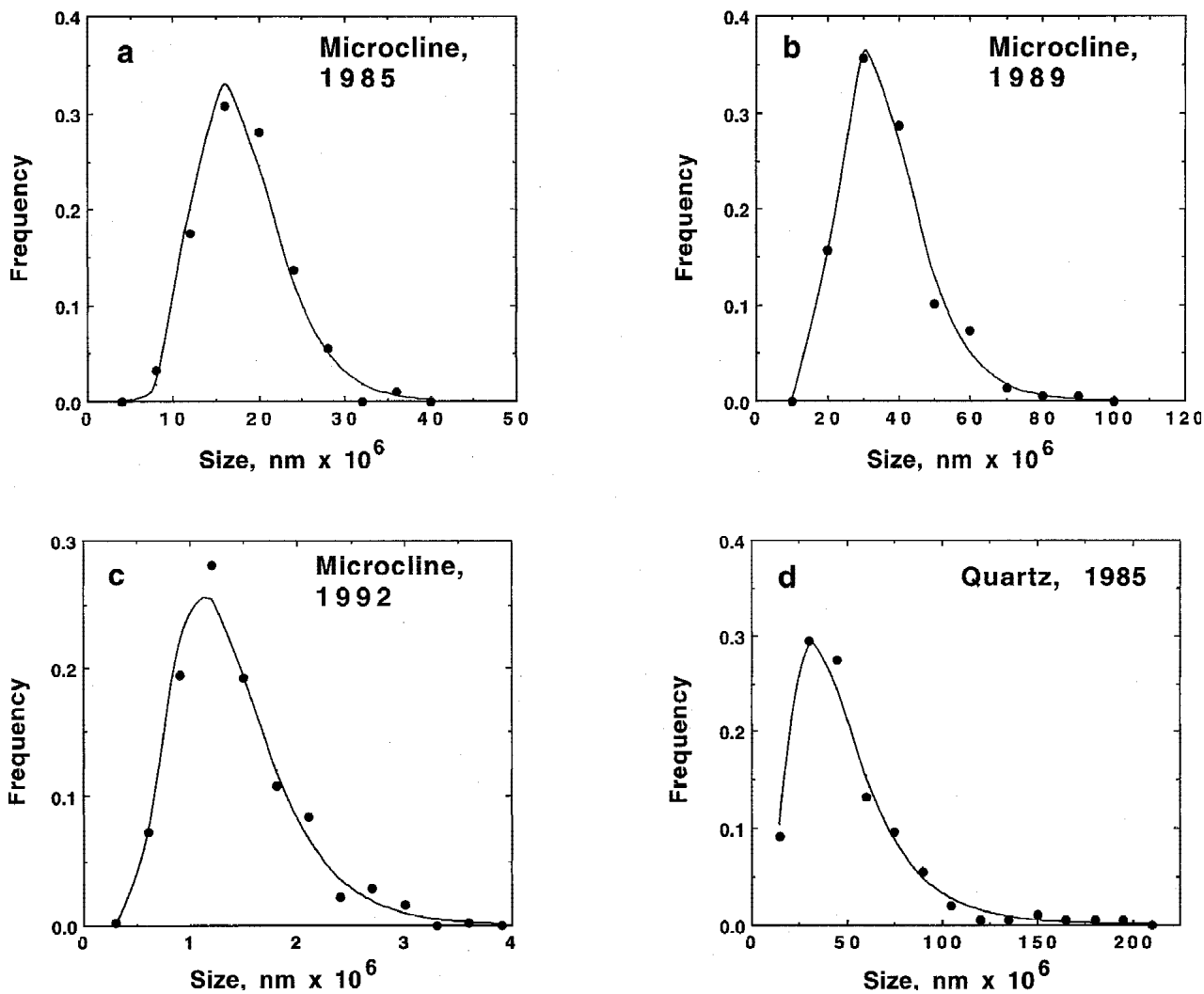

FIGURE 2. Representative plots showing CSDs superimposed on the theoretical lognormal curves (solid lines): **(a)** microcline, LGR, 1985; **(b)** microcline, LGR, 1989; **(c)** microcline, north of LGR, 1992; and **(d)** quartz, LGR, 1985.

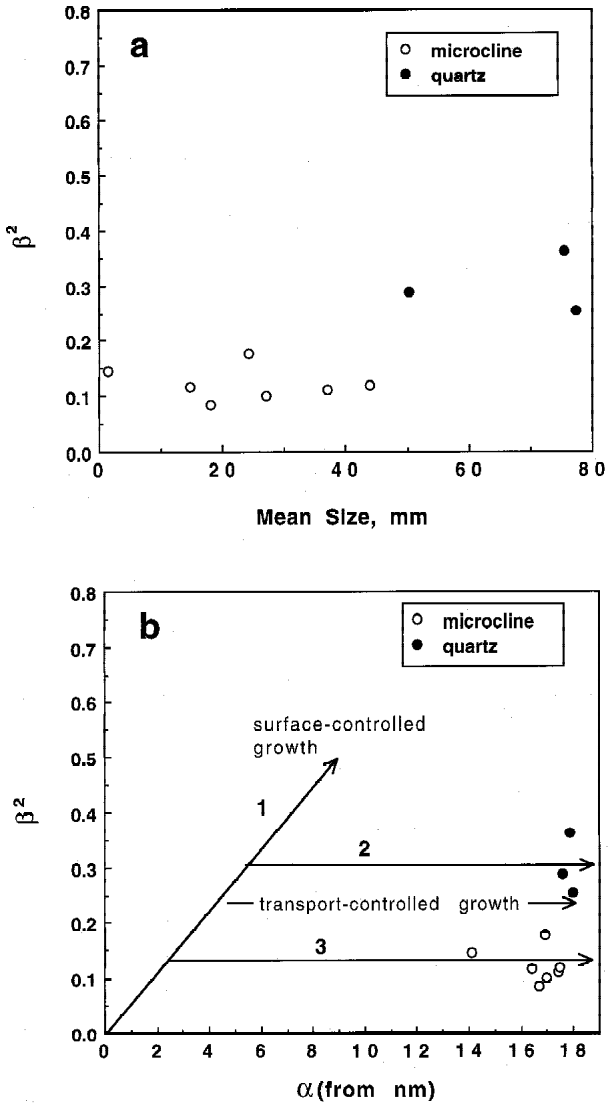

FIGURE 3. (a) Plot of β^2 (size variance) vs. mean crystal size (mm) for pegmatites studied. **(b)** Plot of β^2 (size variance) vs. α (log mean size, calculated from nanometers) for pegmatites studied.

PROPOSED CRYSTAL GROWTH MECHANISMS

The shapes of such CSDs and their evolution can be predicted from the crystal growth model proposed by Eberl et al. (1998), in which crystal growth is influenced both by growth dispersion and by size dependent growth, as is embodied by the Law of Proportionate Effect (LPE; Kapteyn 1903):

$$X(j+1) = X(j) + \varepsilon(j)X(j) \quad (4)$$

where X(j+1) is the size of a crystal after (j+1) growth cycles. System variability, $\varepsilon(j)$, is a random number that varies between 0 and 1, and reflects microscopic system heterogenities, such as thermal and chemical fluctuations, density of growth sites on crystal surfaces, ranges in porosity and permeability, and other variables that may influence crystal growth when a system is far from equilibrium.

When Equation 4 is iterated for many (1001) crystals for several growth cycles using the computer program GALOPER (Growth According to the Law of Proportionate Effect and by Ripening; Eberl et al. 1998), a lognormal distribution results. The LPE is the only calculation known to the authors that generates a lognormal size distribution from the growth of linear crystal dimensions. An alternative approach using the gamma function also fits the crystal size data (Randolph and Larson 1988; Vaz and Fortes 1988). This function can be generated by simultaneous nucleation of randomly spaced particles that grow at a constant rate until the space is completely filled, resulting in a Voronoi partition and a gamma size distribution (Weaire et al 1986; Vaz and Fortes 1988). In accordance with this model, size dispersion results from growth interference. However, this concept seems not to apply to crystallization within a miarolitic cavity, where crystals grow freely from cavity walls into an aqueous vapor medium and generally do not entirely fill the cavity. If the Voronoi partition was the basis for the growth model, then all cavity crystals (without growth interference) should have the same size. Thus, the LPE is inferred to be the initial growth law for microcline and quartz crystals. Most other crystal growth models assume that crystals have a constant growth rate that is independent of size, and, therefore, these models cannot readily reproduce the lognormal size distributions observed in many naturally occurring crystal populations.

However, if LPE growth was the only mechanism operating, then GALOPER calculations indicate that β^2 would increase linearly with α (path 1 in Fig. 3b), whereas the experimental data (Table 1) indicate that β^2 remains relatively constant as size increases. This problem can be reconciled if one applies a mass (volume) balance constraint to crystal growth after the lognormal profile has been established (Eberl et al. 1998), thereby changing the crystal growth mechanism from unconstrained surface-controlled growth to constrained supply controlled growth. The latter growth mechanism is constrained by the total volume available for growth ($\sum \Delta V_a$; this value is entered into the program) for all 1001 crystals during each calculation cycle of Equation 4.

The increase in volume for each crystal (ΔV_j) during each calculation cycle is given by:

$$\Delta V_j = \left(\Delta V_{j,LPE}\right) \frac{\sum \Delta V_a}{\sum \Delta V_{j,LPE}} \quad (5)$$

The crystals first are allowed to grow freely during a GALOPER calculation cycle according Equation 4. Next the growth volume for that cycle for each crystal is calculated ($\Delta V_{j,LPE}$), and the growth volumes for all crystals are summed ($\sum \Delta V_{j,LPE}$). The unconstrained growth volume for each crystal then is reduced proportionately by the ratio of available volume ($\sum \Delta V_a$) to unconstrained growth volume. The corrected growth volume for each crystal (ΔV_j) is added to the previous volume of the crystal, and a new diameter for each crystal for that growth cycle then is calculated from the equation for the volume of a sphere. The calculation is repeated for each growth cycle. Therefore, during this type of growth the LPE is still the growth law, but growth is limited proportionately by supply.

Such a volume constraint has the mathematical effect of greatly reducing the range of system variability, $\varepsilon(j)$, in Equa-

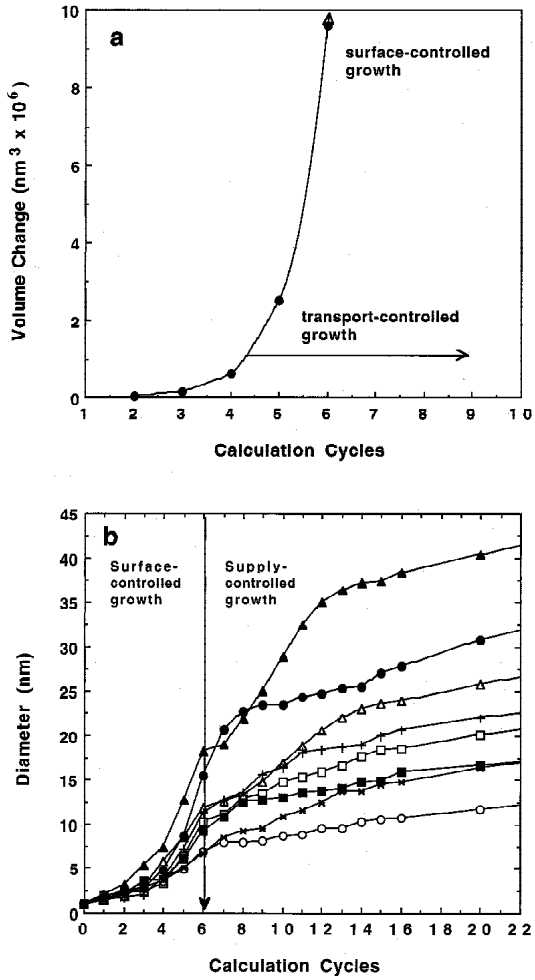

FIGURE 4. (a) Plot of volume increase vs. growth cycles calculated by GALOPER (Eberl et al. 1998), illustrating the exponential increase in volume required by LPE growth as the number of calculation cycles (i.e., reaction time) increases. **(b)** Growth trajectories for 8 crystals calculated using the program GALOPER (Eberl et al. 1998). Supply-controlled growth begins to express itself after 6 cycles of Equation 4, where growth is constrained to a maximum volume increase of 10^6 nm^3 for each cycle for 1001 spherical crystals.

tion 4. According to this approach, the lognormal shape of the CSD was established early in the growth history of the crystals at a high level of supersaturation, when growth rate was not limited by the supply of nutrients to the crystal surface (i.e., the crystals grew by surface-controlled growth). As the crystals grew larger, the level of supersaturation may have dropped, and the demand of the crystals for nutrients increased exponentially, which is a condition of unconstrained LPE growth. Eventually, supply could not keep up with demand and the crystal growth mechanism changed from surface- to supply (or transport-) controlled growth. The latter growth mechanism would preserve the lognormal shape of the CSD (Fig. 3b, paths 2 and 3). β^2 remained constant as mean crystal size increased, because all of the crystals grew at approximately the same rate. Analogous results were seen in synthetic crystallization experiments by Satoh et al. (1997) where during supply limited growth, the size variance (i.e., standard deviation) of particle size distributions remained constant, independent of mean crystal size.

According to the proposed model, the levels of supersaturation in crystallizing systems may have been variable, but above a certain supersaturation limit surface-controlled growth prevailed, whereas below this limit crystals grew by supply control. The level of supersaturation for this shift in growth mechanism would be partly a function of maximum crystal growth rate and mean crystal size, both of which would change as crystal growth proceeds. When crystals reach a certain size it is impossible for surface-controlled growth to continue because an exponentially increasing demand by the crystals for nutrients eventually overtakes diffusion limitations of the system. This situation is illustrated in Figure 4.

Figure 4a shows crystal volume change for 1001 crystals calculated over several growth cycles (which may or may not be related linearly to reaction time) of Equation 4 using the GALOPER program. This figure illustrates the exponential increase in crystal volume (i.e., mass) with calculation cycles that is a consequence of sustained surface-controlled growth. Figure 4b illustrates growth trajectories for eight individual crystals, taken from a population of 1001 crystal diameters calculated using the GALOPER program, in which the diameters of spherical crystals are plotted as a function of calculation cycles of Equation 4. All crystals have an initial diameter of 1 nm. Size dispersion and size dependent growth result from iteration of Equation 4, i.e., the growth trajectories initially diverge, with the larger crystals tending to grow faster. Analogous results have been reported by White and Wright (1971) for sucrose crystals, and size-dependent growth for several systems also has been noted by Randolph and Larson (1988).

After six calculation cycles, the increase in growth volume for each subsequent calculation cycle is constrained to 10^6 nm^3, which is approximately equal to the total volume of the 1001 crystals after six cycles. Growth rate then decreases and gradually becomes constant for all crystals as the number of cycles increases (i.e., the trajectories are approximately parallel after about 16 cycles), with the largest crystals taking the longest time to reach a constant growth rate. Thus, a consequence of supply controlled growth is that an approximately constant growth rate develops for all crystals. This aspect of the simulation corresponds to observations of Berglund et al. (1983), who noted constant growth rates for individual KNO_3 crystals.

The relatively invariant β^2 for microcline CSDs (Fig. 3) may indicate that LPE growth changed to supply controlled growth at approximately the same mean crystal size within each miarolitic cavity; this size appears to be independent of the mean crystal size ultimately attained, as would be expected for crystals having an exponentially increasing demand for nutrients that grew in solutions having roughly similar levels of supersaturation. Assuming an initial diameter of about 1 nm for microcline crystals from the nucleation step (a size arbitrarily chosen to be slightly larger than that of the unit cell), supply controlled growth began at an α of about 2.2 (Fig. 3b), or at a mean size of approximately 10 nm based on the growth model described above.

The somewhat larger values of β^2 for quartz crystals than for microcline crystals may result from the greater solubility

Table 2. Parameters for lognormal or approximately lognormally shaped CSDs from the literature

Mineral	α	β^2	Mean crystal size (μm)	Reference
chromite	11.5	0.41	110	Waters and Boudreau (1996)*
dolomite	5.9	0.23	0.42	Gregg et al. (1992)
galena	10.4	0.31	38	Stanton and Gorman (1968)
garnet	13.1	0.15	513	Cashman and Ferry (1988)
garnet	13.4	0.13	753	Denison and Carlson (1997)†
ice	14.0	0.30	1390	Colbeck (1986)
sphene	12.1	0.24	209	Kretz (1966)

Notes: Calculation of α and β^2 values based on crystal size expressed in nanometers.
* Value based on average of determinations from two different sample populations.
† Value based on average of determinations from three different sample populations.

of quartz; alternatively, it could result from inhibited nucleation of the SiO_2 phase, resulting in higher levels of supersaturation and consequent extended surface-controlled growth after nucleation, or from a slower maximum growth rate for quartz crystals. Surface-controlled LPE growth could therefore be sustained longer for quartz (Fig. 3b, path 2) than for microcline (Fig. 3b, path 3), and β^2 would thus be larger when supply controlled growth began.

A similar supply controlled growth mechanism for crystal growth is noted in zinnwaldite crystals within these same miarolitic cavities. Some of these crystals show hundreds of distinct color or optical zones (Kile and Foord 1998), which are presumed to result from diffusion-related phenomena, a manifestation of supply controlled growth that is in accordance with the crystal growth model proposed here for microcline and quartz. Numerous other examples of diffusion-controlled oscillatory zoning and presumably diffusion-controlled crystal growth are noted in naturally occurring crystals from diverse environments, for example plagioclase, pyroxenes, zircon, and garnet, among others.

A mechanism involving surface-controlled LPE growth, followed by supply controlled growth, is consistent with lognormal CSDs and comparatively low β^2 values found for many other naturally occurring crystals from diverse geological environments (Table 2). The average value of β^2 for these samples is 0.25, compared to an average β^2 for microcline of 0.12, and for quartz of 0.30. Given the proposed short duration of LPE growth during which size variance is established, it is not unexpected that many natural occurrences would show a small β^2. The small size variance noted for microcline and quartz from LGR occurrences indicates that crystallization took place from a single nucleation event; a second nucleation event would result in a bimodal CSD, whereas continuing nucleation would be expected to result in a larger β^2 and in multiple generations of crystals. These observations are suggestive of relatively constant geologic conditions (i.e., temperature, pressure, chemical fluctuation, etc.) during early stages of crystallization.

COMPARISON WITH OTHER PROPOSED CRYSTAL GROWTH MECHANISMS

Most other mechanisms that describe crystal growth (e.g., Mahin et al. 1980; Frost and Thompson 1987; Nielson 1964; Nordeng and Sibley 1966; Joesten 1991; Kerrick et al. 1991; Carlson et al. 1995; Marsh 1988; Marsh 1997) assume that all crystals grow at the same linear rate throughout their growth history. A consequence of this assumption of linear growth rate is that the shapes of the CSDs are controlled by differential nucleation. For example, the positively skewed shapes in Figure 2 would result from an initially slow nucleation rate, which would explain the right tails of the distributions, followed by an increasing nucleation rate that reaches a peak and then rapidly dies off, thereby accounting for the maxima and the short left tails. After such nucleation events, the shapes of the distributions would be maintained during subsequent growth because all crystals grow at the same rate. However, the data presented here (Table 1) favor LPE growth, because it is unlikely that a mechanism based on differential nucleation and a constant growth rate (DNCG) would lead, by chance and in most cases, to lognormal CSDs. LPE growth, however, demands lognormality.

It is important to distinguish the correct growth law because geological interpretations differ greatly between models. For example, the DNCG approach requires that the largest crystals on the right sides of the CSDs (Fig. 2) are the oldest, and that crystals decrease in age with decreasing size. With LPE growth, however, all crystals could have nucleated simultaneously (although simultaneous nucleation is not a necessary condition for developing lognormal CSDs; see Eberl et al. 1998). With subsequent LPE growth, the larger crystals attract more new material during the initial LPE growth stage. Whereas the DNCG model indicates that nucleation rates can be inferred from the shapes of the CSDs (e.g., Waters and Boudreau 1996; Lasaga 1998), the LPE growth mechanism suggests that the CSD shape carries little information about nucleation rates.

The present approach also indicates that the CSD shape carries limited information about physico-chemical conditions during crystal growth, as evidenced by similar CSD shapes that are found for minerals as diverse as ice and garnet (Table 2). However, determination of crystal growth mechanism from CSD shape may be the first step in understanding what physical and chemical data mean in terms of environmental conditions during mineral formation. For example, to discover crystal growth histories by isotopic analysis of separate particle sizes or of zones within crystals, one must know which of the crystal growth mechanisms prevailed.

If the crystal growth mechanism is governed by the LPE, then Equation 4 indicates that little can be learned from the shape of the CSD concerning individual, microscopic variables that influence crystal growth rates. Crystal growth is driven by $\varepsilon(j)$, which is a random variable that is independent of crystal size, and if these conditions concerning $\varepsilon(j)$ are not met, then a lognormal distribution will not result. In other words, interactions between chemical variables on the microscopic scale are so complex that they can be described by a random number. Equation 4 predicts that if a crystal grew fast during a previous period of time, then a similar set of unspecified forces and conditions may tend to operate on it in the future to cause it to continue to grow fast. This approach gives a poor prediction concerning relative growth rates for individual crystals but is very good for predicting relative growth rates for distributions of crystals.

SUMMARY AND CONCLUSIONS

Evaluation of the mean size, variance, and shapes of crystal size distributions provides a method for assessing crystal growth mechanisms in geological systems. The lognormal CSDs of amazonite and smoky quartz crystals from miarolitic pegmatites of the LGR may indicate that growth occurred initially by surface-controlled kinetics (LPE growth), during which lognormal CSD shapes were established very early in the crystallization history. A small and relatively constant β^2 for the CSDs over a wide range of mean crystal sizes, may indicate subsequent supply controlled (e.g., diffusion-limited) growth throughout the remaining crystallization. This hypothesis for crystal growth accounts for the relative scarcity (and corresponding high monetary value) of natural crystal specimens that have a wide range of crystal sizes.

ACKNOWLEDGMENTS

The authors express thanks to Peter J. Modreski and John M. Neil (U.S. Geological Survey), Karen L. Webber (University of New Orleans), Thomas Dewers (University of Oklahoma), and an anonymous reviewer for their review and constructive comments of this manuscript. We also thank John R. Muntyan for photographing the specimen shown in Figure 1b.

REFERENCES CITED

Benjamin, J.R. and Cornell, C.A. (1970) Probability and decision for civil engineers, 684 p. McGraw-Hill Book Co., New York.

Berglund, K.A., Kaufman, E.L., and Larson, M.A. (1983) Growth of contact nuclei of potassium nitrate. American Institute of Chemical Engineers Journal, 29, 867–869.

Bryant, B., McGrew, L.W., and Wobus, R.A. (1981) Geologic map of the Denver 1° × 2° quadrangle, north-central Colorado. U.S. Geological Survey Map I–1163. U.S. Government Printing Office, Washington, D.C.

Carlson, W. D., Denison, C., and Ketcham, R. A. (1995) Controls on the nucleation and growth of porphyroblasts: kinetics from natural textures and numerical models. Geological Journal, 30, 207–225.

Cashman, K.V. and Ferry, J.M. (1988) Crystal size distribution (CSD) in rocks and the kinetics and dynamics of crystallization. III. Metamorphic crystallization. Contributions to Mineralogy and Petrology, 99, 401–415.

Cashman, K.V. and Marsh, B.D. (1988) Crystal size distribution (CSD) in rocks and the kinetics and dynamics of crystallization. Part II: Makaopuhi lava lake. Contributions to Mineralogy and Petrology, 99, 292–305.

Colbeck, S.C. (1986) Statistics of coarsening in water-saturated snow. Acta Metallurgica, 34, 347–352.

Denison, C. and Carlson, W.D. (1997) Three-dimensional qualitative textural analysis of metamorphic rocks using high-resolution computed X-ray tomography: Part II. Application to natural samples. Journal of Metamorphic Geology, 15, 45–57.

Dowty, E. (1980) Crystal growth and nucleation theory and the numerical simulation of igneous crystallization. In R.B. Hargraves, Ed., The physics of magmatic processes, p. 419–485. Princeton Press, Princeton.

Eberl, D.D., Drits, V.A., and Środón, J. (1998) Deducing growth mechanisms for minerals from the shapes of crystal size distributions. American Journal of Science, 298, 499–533.

Frost, H. J. and Thompson, C. V. (1987) The effect of nucleation conditions on the topology and geometry of two-dimensional grain structures. Acta Metallurgica, 35, 529–540.

Gregg, J.M., Howard, S.A., and Mazullo, S.J. (1992) Early diagenetic recrystallization of Holocene (<3000 years old) peridital dolomites, Ambergris Cay, Belize. Sedimentology, 39, 143–160.

Joesten, R. L. (1991) Kinetics of coarsening and diffusion-controlled mineral growth. Mineralogical Society of America Reviews in Mineralogy, 26, 507–582.

Kapteyn, J.C. (1903) Skew Frequency Curves in Biology and Statistics: Noordhoff, Groningen, Astronomical Laboratory, 69 p.

Kerrick, D. M., Lasaga, A. C., and Raeburn, S. P. (1991) Kinetics of heterogeneous reactions. Mineralogical Society of America Reviews in Mineralogy, 26, 583–671.

Kile, D.E. and Foord, E.E. (1998) Micas from the Pikes Peak batholith and its cogenetic pegmatites, Colorado: Optical properties, composition, and correlation with pegmatite evolution. Canadian Mineralogist, 36, 463–482.

Kirkpatrick, R.J. (1981) Kinetics of crystallization of igneous rocks. In Mineralogical Society of America Reviews in Mineralogy, 8, 321–398.

Koch, G.S. Jr. and Link, R.F. (1971) Statistical analysis of geological data, vol. 1, p. 215. Dover Publications, New York.

Kretz, R. (1966) Grain-size distribution for certain metamorphic minerals in relation to nucleation and growth. Journal of Geology, 74, 147–173.

Krumbein, W. C. and Graybill, F. A. (1965) An introduction to statistical models in geology. 475 p. McGraw-Hill Book Co., New York, .

Larson, M.A., White, E.T., Ramanarayanan, K.A., and Berglund, K.A. (1985) Growth rate dispersion in MSMPR crystallizers. American Institute of Chemical Engineers Journal, 31, 90–94.

Lasaga, A.C. (1982) Crystal growth from silicate melts. American Journal of Science, 282, 1264–1288.

——— (1998) Kinetic theory in the Earth sciences. 811 p. Princeton University Press, Princeton.

Mahin, K.W., Hanson, K., and Morris, J.W. Jr. (1980) Comparative analysis of the cellular and Johnson-Mehl microstructures through computer simulation. Acta Metallurgica, 28, 443–453.

Marsh, B.D. (1988) Crystal size distribution (CSD) in rocks and the kinetics and dynamics of crystallization Part I: Theory. Contributions to Mineralogy and Petrology, 99, 277–291.

——— (1998) On the interpretation of crystal size distributions in magmatic systems. Journal of Petrology, 39, 553–599.

Mullin, J.W. (1974) Bulk crystallization. In B.R. Pamplin, Ed., Crystal growth. 2nd ed., p. 289–335. Pergamon Press, New York.

Nielson, A. E. (1964) Kinetics of precipitation. 151 p. Pergamon, New York.

Nordeng, S.H. and Sibley, D.F. (1996) A crystal growth equation for ancient dolomites: Evidence for millimeter-scale flux-limited growth. Journal of Sedimentary Research, 66, 477–481.

Ohara, M. and Reid, R.C. (1973) Modeling crystal growth rates from solution. 272 p. Prentice-Hall, New Jersey.

Randolph, A.D. and Larson, M.A. (1988) Theory of particulate processes. 2nd ed. Academic Press, New York. 369 p.

Satoh, T., Akitaya, M., Konno, M., and Saito, S. (1997) Particle size distributions produced by hydrolysis and condensation of tetraethylorthosilicate. Journal of Chemical Engineering of Japan, 30, 759–762.

Stanton, R.L. and Gorman, H. (1968) A phenomenological study of grain boundary migration in some common sulfides. Economic Geology, 63, 907–923.

Unruh, D.M., Snee, L.W., Foord, E.E., and Simmons, W.B. (1995) Age and cooling history of the Pikes Peak batholith and associated pegmatites. Geological Society of America, Abstracts with Programs, 27, A–468.

Vaz, M.F. and Fortes, M.A. (1988) Grain size distribution: The lognormal and the gamma distribution functions. Scripta Metallurgica, 22, 35–40.

Waters, C. and Boudreau, A.E. (1996) A reevaluation of crystal-size distributions in chromite cumulates. American Mineralogist, 81, 1452–1459.

Weaire, D., Kermode, J.P., and Wejchert, J. (1986) On the distribution of cell areas in a Voronoi network. Philosophical Magazine B, 53, L101–L105.

White, E.T. and Wright, P.G. (1971) Magnitude of size dispersion effects in crystallization. In M.A. Larson, Ed., Crystallization from solution: factors influencing size distribution. American Institute of Chemical Engineers, 81–87.

Wobus, R.A. and Anderson, R.S. (1978) Petrology of the Precambrian intrusive center at Lake George, southern Front Range, Colorado. U.S. Geological Survey Journal of Research, 6, 81–94. U.S. Government Printing Office, Washington, D.C.

Wobus, R.A. and Hutchinson, R.M. (1988) Proterozoic plutons and pegmatites of the Pikes Peak region, Colorado. In G.S. Holden, Ed., Field Trip Guidebook. Professional Contributions no. 12, 35–42. Colorado School of Mines, Golden.

MANUSCRIPT RECEIVED AUGUST 17, 1998
MANUSCRIPT ACCEPTED DECEMBER 12, 1998
PAPER HANDLED BY DAVID LONDON